# ELECTRONIC SUPPLEMENTARY INFORMATION

# Cu-loaded zeolites enable the selective activation of ethane to ethylene at low temperature and pressure

Karoline Kvande,[a] Sebastian Prodinger,[a] Bjørn Gading Solemsli,[a] Silvia Bordiga,[b] Elisa Borfecchia,[b] Unni Olsbye,[a] Pablo Beato,[c] and Stian Svelle.[a,*]

[a] Center for Materials Science and Nanotechnology (SMN), Department of Chemistry, University of Oslo, 1033 Blindern, 0315, Oslo, Norway.

[b] Department of Chemistry, NIS Center and INSTM Reference Center, University of Turin, via P. Giuria 7, 10125 Turin, Italy

[c] Topsoe A/S, Haldor Topsøes Allé 1, DK-2800 Kgs. Lyngby, Denmark

*Correspondence:
stian.svelle@kjemi.uio.no (S.S.)

## Innholdsfortegnelse



## 1. Experimental section

### 1.1. Material preparation and characterization

Cu-zeolites with different composition and cations have been investigated for the reaction. The nomenclature of the zeolite samples is yCu,x-ZEOLITE(z), where y is the Cu/Al ratio of the sample, x is the cation present, either H or Na, and z is the Si/Al ratio of the zeolite. The zeolites used herein is either mordenite (MOR), CHA (SSZ-13) or an MFI type framework (ZSM-5). The MOR samples were made from commercially available material from Zeolyst, namely CBV21A (Si/Al = 11) and CBV10Ads (Si/Al = 7). The ZSM-5 sample used for this

study came also from Zeolyst, CBV 2314 (Si/Al = 11.5), while SSZ-13 was prepared in a procedure described elsewhere [1]. In addition to Cu-zeolites, also an H-form of CBV21A (H-MOR(11)) and Cu exchanged $SiO_2$ (ecoChrom MP Silica 100-200, 60 Å) and $SiO_2/Al_2O_3$ (Sigma Aldrich, grade 135, Al = 6.5 %) were tested in the reaction. The Cu-source for $SiO_2$ and $SiO_2/Al_2O_3$ was $Cu(NO_3)_2{\times}3H_2O$ (Sigma Aldrich). A 5wt%-$CuSiO_2$ and 2.5wt%Cu-$SiO_2/Al_2O_3$ sample was prepared following the procedure reported by Prodinger et al. [2], and the Cu wt.% of the samples is determined based on the intended ratio between Cu and SiO2 or aluminium, respectively, before exchange.

Basic characterization of the MOR zeolites have been performed previously and was reported by Dyballa et al. [3] Characterization of 0.34Cu-SSZ-13 is reported by Pappas et al. [4], and characterization of the ZSM-5 sample is reported in a publication by Deplano et al. [5].

### 1.2. Ethane activation measurements

The testing was performed with a customized set-up previously used for the MTM conversion [4, 6-8]. 100 mg sample (~85 mg of dry weight, sieve fraction: 425 – 250 µm) was placed inside a straight quartz tube reactor (i.d. = 6 mm). The temperature of the oven was calibrated prior to the measurements using a thermocouple inside a quartz sheet on top of the reactor bed. The flow of gases was controlled using four different MFCs and fed separately onto the sample with the help of stop- and 4-way valves. The activity of the materials towards ethane activation was tested with a very similar protocol to the optimized stepwise conversion route for MTM [4]. For the standard protocol, the only difference to what has been reported previously was a lower temperature for $C_xH_y$ loading and subsequent water extraction from 200 to 150 °C. A shorter $C_2H_6$ loading time (210 min instead of 360 min) was also utilized, similar to our latest work within the MTM reaction [7, 9]. Scheme S1 represents the optimized protocol for the MTM process reported for CHA by Pappas et al [4], and the ethane activation protocol (ETE) applied herein. The reaction protocol involves three main steps. First, the sample is activated in $O_2$ (100 %) 500 °C for 8 h. Then the reaction temperature is lowered to 150 °C (5 °C/min) and flushed with He for 1 h, before $C_2H_6$ (5 %/rest. He) was introduced for 210 min. A second flushing step was performed in He, before a water-saturated 10 % Ne/He stream was introduced isothermally. The saturator was heated to 45 °C to obtain ~ 10 % water in the feed. All flows were kept to 15 ml/min. The effluent was monitored with an online quadrupole mass spectrometer (Omnistar GSD320, Pfeiffer). For quantitative analysis of the main product, a microgas chromatograph (µGC 3000A, Agilent) equipped with a Plot U column with an FID detector and He as the carrier gas, was employed.

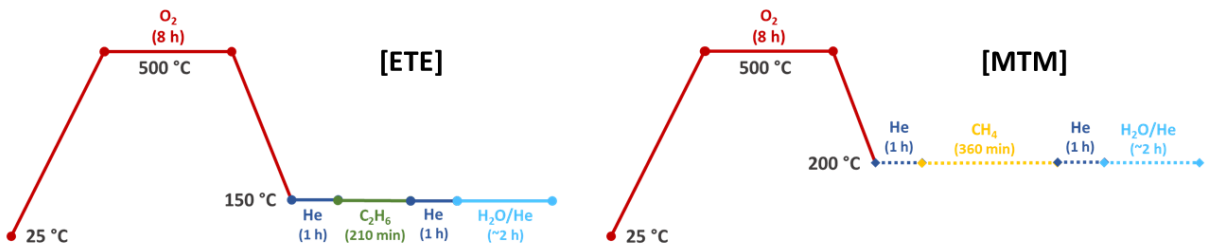


**Scheme S1.** Reaction protocol for the ETE protocol applied herein and the previously applied MTM process on the materials.

### 1.3. Fourier Transform Infrared (FT-IR) spectroscopy

FT-IR spectroscopy was performed on a Bruker Vertex 70 instrument with a Mercury-Cadmium-Telluride (MCT) detector. The interaction of ethylene adsorption on the 0.36CuMOR11 and H-MOR11 samples at RT was investigated. Each sample was pressed with 2-3 tons into self-supporting wafers (11.3 mg/cm$^2$) and fitted inside gold envelopes. The envelopes were placed in a low temperature vacuum cell with KBr windows and heated under vacuum at 450 °C for 1.5 h (ramp rate = 5 °C/min) for pretreatment. After cooling to RT, individual spectra were collected while small amounts of ethylene were dosed onto the sample, until reaching an equilibrium pressure of 17 mbar. After dosing, the sample was also cooled with LN2, before it was slowly outgassed and consecutively heated back to RT. FT-IR spectra were collected during all parts of the experiment.

## 2. Material summary

For the purpose of this study, a library of well-studied Cu-zeolites in the MTM reaction were chosen in order to be able to directly compare the effect of the reaction protocols. Table S1 summarizes the characteristics of all samples.

**Table S1.** Chemical composition and MTM performance of the materials used herein.

| Sample name | Si/Al | Cu/Al | Cu wt.% | MTM Productivity ($mol_{MeOH}/mol_{Cu}$) | MTM Yield ($\mu mol_{MeOH}/g_{zeolite}$) |
|---|---|---|---|---|---|
| **H-MOR(11) [1)]** | 11 | - | - | - | - |
| **0.19Cu,H-MOR(11) [1)]** | 11 | 0.19 | 1.67 | 0.24 | 64 |
| **0.36Cu,H-MOR(11) [1)]** | 11 | 0.36 | 3.18 | 0.25 | 123 |
| **0.32Cu,Na-MOR(11) [1)]** | 11 | 0.32 | 2.83 | 0.17 | 74 |
| **0.18Cu,H-MOR(7) [1)]** | 7 | 0.18 | 2.33 | 0.47 | 172 |
| **0.35Cu,H-ZSM-5(11) [2)]** | 11.5 | 0.35 | 2.88 | 0.10 | 43 |
| **0.30Cu,H-SSZ-13(12)[1)]** | 12.1 | 0.34 | 2.68 | 0.16 | 67 |
| **2.5wt%-Cu/SiO2/Al2O3** | 14.6 | 0.38 | 2.5 | - | - |
| **5wt%-$CuSiO_2$** | - | - | 5 | - | - |

1) Elemental composition, such as Si/Al, Cu/Al and Cu wt.%, along with the MTM productivity and yield of the Cu-exchanged MOR zeolites and the 0.30Cu,H-SSZ-13(1) sample have been determined by Svelle and co-workers in previous publications [3, 4, 6]. The protocol for MTM is reported in Scheme S1.
2) The MTM activity of 0.35Cu,H-ZSM-5(11) was measured herein with the instrumentation and protocol reported in our previous study by Prodinger et al. [9]. Elemental composition, such as Si/Al, Cu/Al and Cu wt.% was previously reported by Deplano et al. [5].

## 3. Product selectivity derived from GC-FID

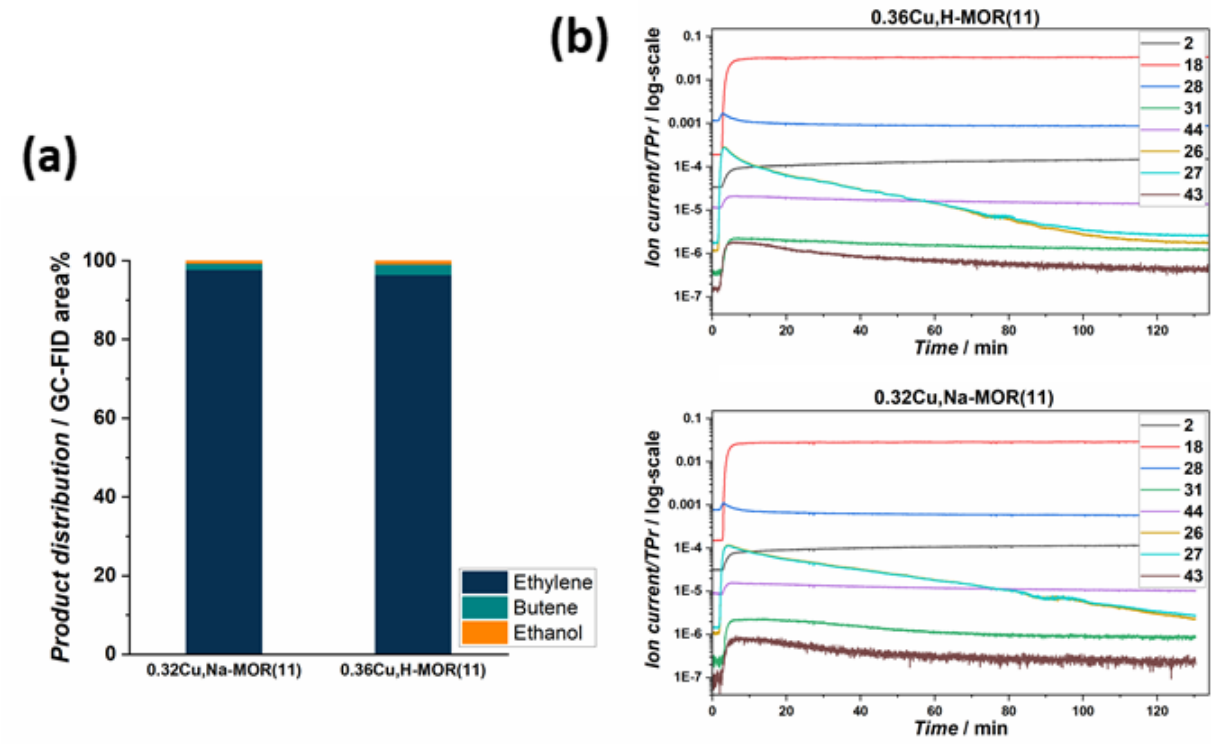


**Figure S1.** Bar plot (a) comparing the product distribution during the ETE protocol reported in Scheme 1 in the main text as observed by GC-FID for 0.32Cu,Na-MOR(11) and 0.36Cu,H-MOR(11). A selection of mass fragments (b) collected during the water extraction step, as observed by an online MS is reported. The y-axis represents ion current divided by the total pressure of the mass spectrometer in log-scale, and the time in minutes (min) is reported on the x-axis from right after water was introduced to the reactor.

## 4. FT-IR spectroscopy

To see the remaining Brønsted acid sites in 0.32Cu,Na-MOR(11) compared to 0.36Cu,H-MOR(11), and the pure H-MOR zeolite, the FT-IR spectra of vacuum activated (450 °C) samples were compared. Figure S2 shows the normalized ν(O-H) stretch region, and the band at 3610 $cm^{-1}$ is linked with the ν(O-H) stretch of Brønsted acid sites (Si-(O-H)-Al).

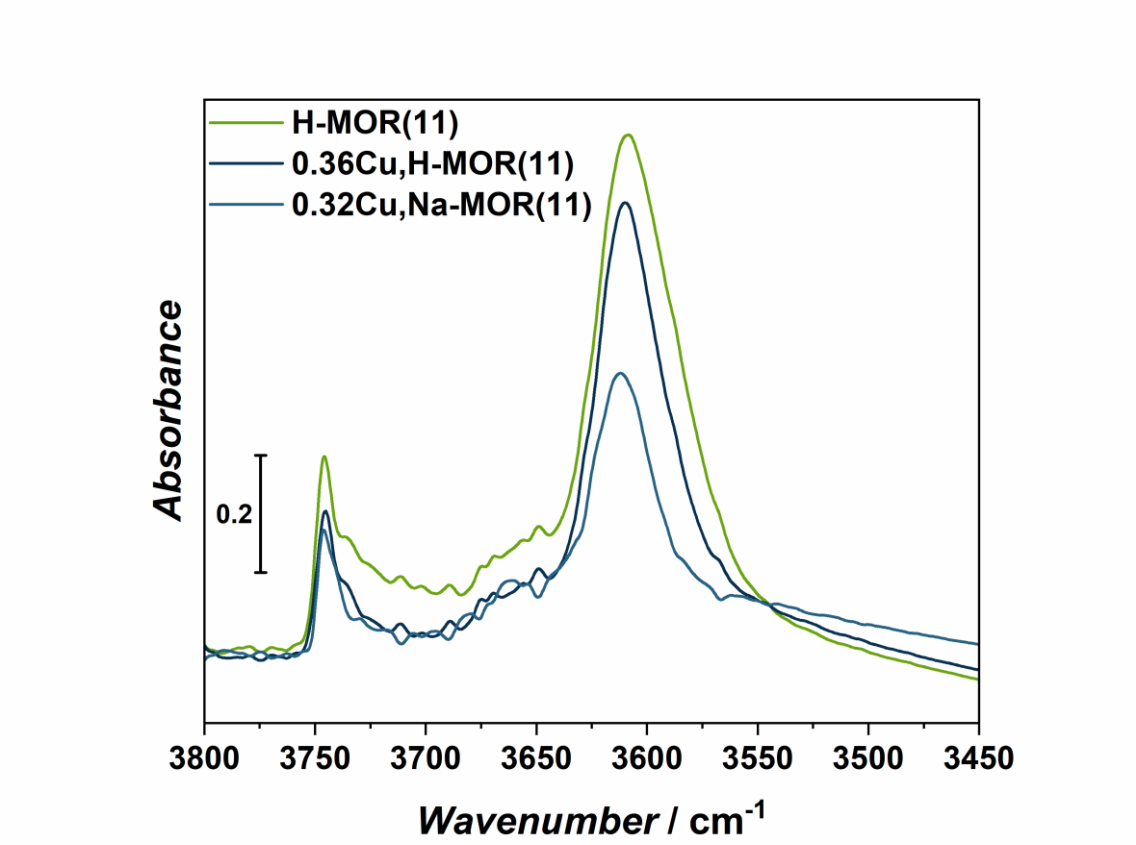


**Figure S2.** FT-IR spectra of the ν(O-H) stretch region of 0.32Cu,Na-MOR(11), 0.36Cu,H-MOR(11), and H-MOR(11).

In both 0,36Cu,H-MOR(11) and H-MOR, the features related to gaseous ethylene appear quite fast, as observed from the strong symmetric stretching band of $CH_2$ at 2989 $cm^{-1}$. However, the band appearing at 2982 $cm^{-1}$ is likely a downward shift of the same functional group, confirming that the $C_2H_4$ gas is also perturbed by the framework by forming a $C_2H_4$-OH π-complex [10]. This is also evident by the shift to lower frequency for the Brønsted ν(O-H) stretching bands (

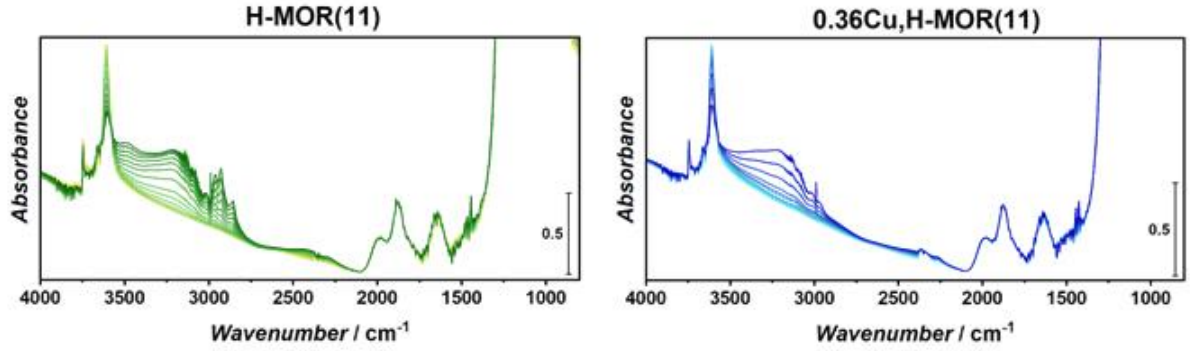


Figure S3) and the band appearing at 1340 $cm^{-1}$, which is a bending mode of CH2 that is IR-inactive in the free molecule (Figure S4). For the ethylene molecule, a second, IR-active, bending mode for $CH_2$ should also be present in the IR spectra. The bands at 1444 and 1428 $cm^{-1}$, as observed in Figure S4, can be attributed to this bend in the free molecule as well as perturbed by $Cu^+$, respectively. Due to spectral noise, it is not possible to separate out any downward shift of the band at 1444 $cm^{-1}$ related to the adsorption on the framework.

Upon scrutinizing the spectra in Figure S4, only small indications of the IR inactive ν(C=C) stretch vibration on Brønsted sites (~ 1612 $cm^{-1}$) are observed [10, 11]. However, as this is almost indistinguishable from the background, the FT-IR spectra obtained under the conditions reported here can unfortunately not be used to search for the ethylene molecules preferential siting (H- or Cu-) inside the Cu-zeolite framework.

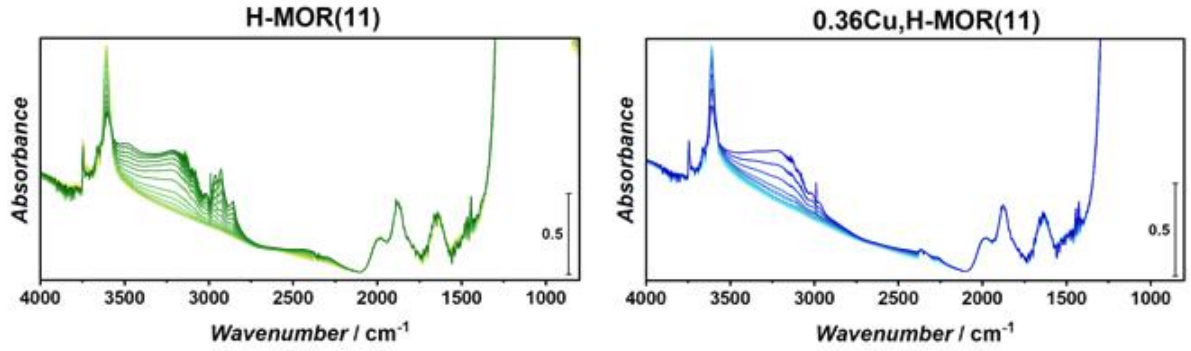


**Figure S3.** FT-IR spectra of the full region obtained for adsorbed ethylene at RT on H-MOR(11) (left panel) and 0.36Cu,H-MOR(11) (right panel). Each spectrum is obtained after sending incremental doses of ethylene onto the sample from about 50 µbar to 17 mbar of equilibrium pressure. Before dosing, the samples were pretreated under vacuum at 450 °C for 1.5 h (ramp rate = 5 °C/min). The spectra are normalized to the framework overtone.

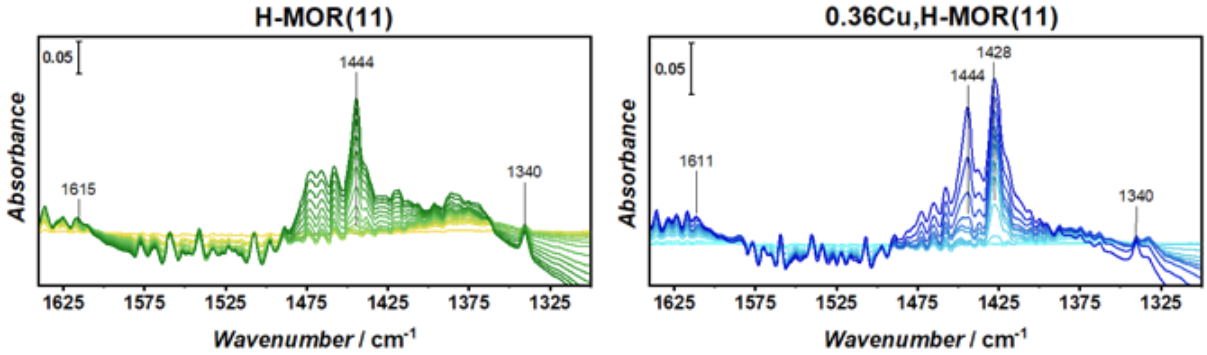


**Figure S4.** FT-IR spectra of the C=C stretch and -CH bend region obtained for adsorbed ethylene at RT on H-MOR(11) (left panel) and 0.36Cu,H-MOR(11) (right panel). Each spectrum is obtained after sending incremental doses of ethylene onto the sample from about 50 µbar to 17 mbar of equilibrium pressure. Before dosing, the samples were pretreated under vacuum at 450 °C for 1.5 h (ramp rate = 5 °C/min). The spectra are normalized to the framework overtone and background subtracted. All additional bands (noise) are due to atmospheric moisture affecting spectra.

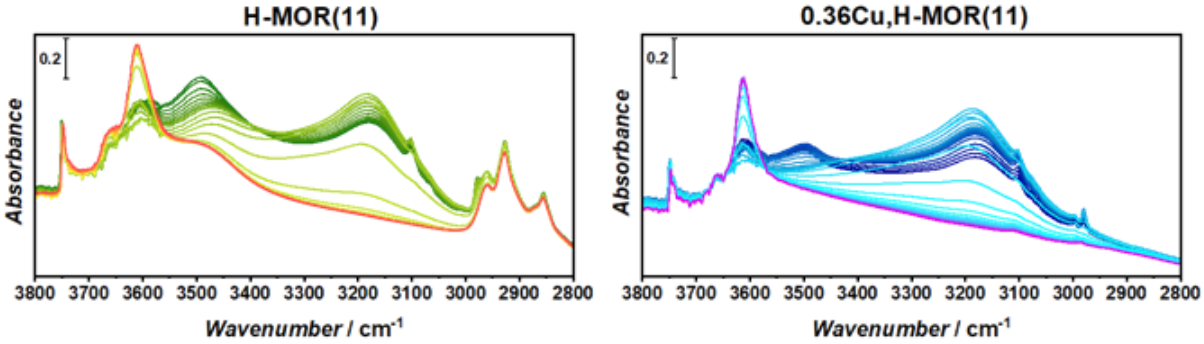


**Figure S5.** FT-IR spectra of the -OH and -CH stretch region showing the desorption of ethylene over time from 100 K to RT. The spectra show which bands are disappearing, and which are remaining upon outgassing and heating to RT. For H-MOR(11) (left panel), dark green spectrum represents the bands present at 100 K, while the orange spectrum represents completely outgassed at RT. For 0.36Cu,H-MOR(11) (right panel), dark blue spectrum represents the bands present at 100 K, while the pink spectrum represents completely outgassed at RT. Before outgassing, the ethylene dosed samples were cooled to 100 K (with $LN_2$).

## 5. References

[1] T. V. W. Janssens, H. Falsig, L. F. Lundegaard, P. N. R. Vennestrøm, S. B. Rasmussen, P. G. Moses, F. Giordanino, E. Borfecchia, K. A. Lomachenko, C. Lamberti, S. Bordiga, A. Godiksen, S. Mossin and P. Beato, *ACS Catal.* **2015**, 5, 2832-2845.
[2] S. Prodinger, M. F. K. Verstreken and R. F. Lobo, *ACS Sustainable Chem. Eng.* **2020**, 8, 11930-11939.
[3] M. Dyballa, D. K. Pappas, K. Kvande, E. Borfecchia, B. Arstad, P. Beato, U. Olsbye and S. Svelle, *ACS Catal.* **2019**, 9, 365-375.
[4] D. K. Pappas, E. Borfecchia, M. Dyballa, I. A. Pankin, K. A. Lomachenko, A. Martini, M. Signorile, S. Teketel, B. Arstad, G. Berlier, C. Lamberti, S. Bordiga, U. Olsbye, K. P. Lillerud, S. Svelle and P. Beato, *J. Am. Chem. Soc.* **2017**, 139, 14961-14975.
[5] G. Deplano, M. Signorile, V. Crocellà, N. G. Porcaro, C. Atzori, B. G. Solemsli, S. Svelle and S. Bordiga, *ACS Appl. Mater. Interfaces* **2022**, 14, 21059-21068.
[6] D. K. Pappas, A. Martini, M. Dyballa, K. Kvande, S. Teketel, K. A. Lomachenko, R. Baran, P. Glatzel, B. Arstad, G. Berlier, C. Lamberti, S. Bordiga, U. Olsbye, S. Svelle, P. Beato and E. Borfecchia, *J. Am. Chem. Soc.* **2018**, 140, 15270-15278.
[7] K. Kvande, D. K. Pappas, M. Dyballa, C. Buono, M. Signorile, E. Borfecchia, K. A. Lomachenko, B. Arstad, S. Bordiga, G. Berlier, U. Olsbye, P. Beato and S. Svelle, *Catalysts* **2020**, 10, 191.
[8] D. K. Pappas, E. Borfecchia, M. Dyballa, K. A. Lomachenko, A. Martini, G. Berlier, B. Arstad, C. Lamberti, S. Bordiga, U. Olsbye, S. Svelle and P. Beato, *ChemCatChem* **2019**, 11, 621-627.
[9] S. Prodinger, K. Kvande, B. Arstad, E. Borfecchia, P. Beato and S. Svelle, *ACS Catal.* **2022**, 12, 2166-2177.
[10] G. Spoto, S. Bordiga, G. Ricchiardi, D. Scarano, A. Zecchina and E. Borello, *J. Chem. Soc. Faraday trans.* **1994**, 90, 2827-2835.
[11] J. Datka and E. Kukulska-Zając, *J. Phys. Chem. B* **2004**, 108, 17760-17766.